

An Effect of Layered Earth on Magnetotelluric Responses of Three-Dimensional Bodies

Hee Joon Kim* and Chol Hoon Hong**

ABSTRACT: The integral equation method is used for magnetotelluric (MT) modeling of a finite inhomogeneity in a two-layered earth. An integral equation relates the incident plane-wave field and the scattering currents in the three-dimensional (3-D) inhomogeneity through the electric tensor Green's function appropriate to a layered earth. This paper describes an effect of overburden and basement on MT responses of 3-D body. The effect of overburden is to reduce the detectability of target, and the reduction of detectability is more apparent for conductive overburden than for resistive one. The effect of basement, on the other hand, may enhance the anomaly due to 3-D body in the upper layer. In case of the resistive basement current perturbations about the body tend to be confined to the more conductive upper layer.

INTRODUCTION

Magnetotelluric (MT) measurements are sensitive to the resistivity structure of the earth, potentially to depths exceeding 100 Km (Vozoff, 1972). Recent advances in instrumentation and data processing have enabled procurement of precise tensor MT data (Gamble et al., 1979; Takasugi et al., 1992). However, the skills necessary to translate these measurements into trustworthy models of subsurface resistivity have been slow in developing, and an overall three-dimensional (3-D) interpretation is still not practical (Wannamaker et al., 1984a).

For over a decade, integral equations approaches have been studied for the scattering of electromagnetic wave from 3-D resistivity structure in the earth (Ting and Hohmann, 1981; Das and Verma, 1982; Wannamaker et al., 1984a). They are the most efficient for modeling one or a few buried prisms and have been valuable for basic physical understanding and for establishing the validity of 1-D and 2-D interpretation of field data (Wannamaker et al., 1984b; Kim and Lee, 1994). Further progress in accuracy and versatility of 3-D integral equation models is achieved by Wannamaker (1991) through an accurate treatment of boundary charge contributions from the surface of a 3-D body.

The importance of overburden layers in determining MT signature over potential ore deposits has been recognized by mining geophysicists for some time. Furthermore, large-scale resistivity structures such as sedimentary basins may reside in an essentially 1-D regional

host determined by particular tectonic environment (Wannamaker et al., 1984a). To illuminate characteristics of MT responses from 3-D bodies in layered earths, we have employed the integral equation algorithm developed by Kim and Lee (1994). Their program can accommodate an arbitrary number of layers but, for simplicity, we have concentrated only a two-layer case. This paper describes an effect of overburden and basement on MT responses of 3-D body.

TENSOR MT RESPONSES

Horizontal electric and magnetic fields at the earth's surface can be related by the frequency domain expression

$$E_x = Z_{xx}H_x + Z_{xy}H_y, \quad (1)$$

and

$$E_y = Z_{yx}H_x + Z_{yy}H_y, \quad (2)$$

or in a concise form

$$\mathbf{E} = [\mathbf{Z}] \cdot \mathbf{H}, \quad (3)$$

where

$$\mathbf{Z} = \begin{pmatrix} Z_{xx} & Z_{xy} \\ Z_{yx} & Z_{yy} \end{pmatrix}, \quad (4)$$

is the impedance tensor, and \mathbf{E} and \mathbf{H} are the electric and magnetic field vectors formed by (E_x, E_y) and (H_x, H_y) , respectively. Each element of the impedance tensor Z_{ij} is transformed to its corresponding apparent resistivity ρ_{ij} and impedance phase ϕ_{ij} by

$$\rho_{ij} = |Z_{ij}|^2 / \mu_0 \omega, \quad (5)$$

*Department of Applied Geology, National Fisheries University of Pusan, Pusan 608-737, Korea

**Research Center of Ocean Industrial Development, National Fisheries University of Pusan, Pusan 608-737, Korea

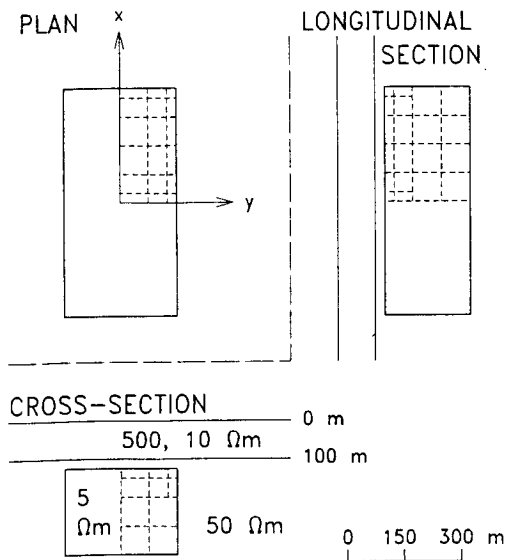


Fig. 1. Prismatic 3-D body in a two-layered earth. Dashes outline the discretization of the conductor into rectangular cells, shown only for the right half of the body in section and upper right-hand quadrant in plan. Overburden resistivities of 500 and 10 $\Omega \cdot m$ are considered.

and

$$\phi_{ij} = \tan^{-1}[\text{Im}(Z_{ij})/\text{Re}(Z_{ij})], \quad i, j = x, y, \quad (6)$$

where $\mu_0 = 4\pi \times 10^{-7}$ is the magnetic permeability, $\omega = 2\pi f$ the angular frequency, $\text{Im}(Z_{ij})$ and $\text{Re}(Z_{ij})$ the imaginary and real parts of Z_{ij} , respectively, and ϕ_{ij} the angle measured counterclockwise in the complex plane. Because the impedance tensor varies with respect to the coordinate system, the apparent resistivity and impedance phase derived from it also vary with the coordinate system.

If the subsurface conductivity is only a function of z , then the impedance measured at the earth's surface can be easily derived. The derivation of the surface impedance is in many standard texts and is not repeated here. The layered-earth impedance Z_i is given by (e.g., Keller and Frischknecht, 1966)

$$Z_i = \frac{i\omega\mu_0}{k_1} \left[\coth k_1 h_1 + \coth^{-1} \left\{ \frac{k_1}{k_2} \coth(k_2 h_2 \dots \right. \right. \\ \left. \left. \left[\coth k_{N-1} h_{N-1} + \coth^{-1} \left(\frac{k_{N-1}}{k_N} \right) \right] \dots \right\} \right] \quad (7)$$

where

$$k_j = (i\omega\mu_0/\rho_j)^{1/2}, \quad (8)$$

and ρ_j and h_j indicate the resistivity and thickness of j th

layer, respectively. Layered-earth apparent resistivity ρ_a and impedance phase ϕ_a can then be obtained from (5) and (6).

A relationship similar to (1) and (2) can be written between magnetic field component H_z and the horizontal magnetic field components H_x and H_y :

$$H_z = AH_x + BH_y, \quad (9)$$

where A and B are unknown complex coefficients, which are called tipper. Its magnitude is given by

$$|T| = (|A|^2 + |B|^2)^{1/2}, \quad (10)$$

EFFECT OF OVERBURDEN RESISTIVITY

Fig. 1 shows a rectangular prism target embedded in a two-layered earth with dimensions $600 \times 300 \times 225$ m buried 125 m beneath the surface. The resistivities of the body and host layer are 5 and 50 $\Omega \cdot m$, respectively, and overburden is 100 m thick. The resistivity of the overburden is varied to study its effect on MT responses. The scattering current within the body was approximated by 52 rectangularly prismatic cells to a quadrant. Contoured MT response functions shown next, with coordinate axes paralleling the axes of symmetry of the body, were derived from 100 variously spaced receiver points per quadrant.

Fig. 2 shows apparent resistivity signatures for the model with resistive overburden (500 $\Omega \cdot m$). Layered-earth apparent resistivities ρ_a , which are given in the upper side of the figure, increase with an increase of frequencies, because the resistivity of overburden is greater than that of lower half-space. The conductive body can be recognized with low apparent resistivity anomalies. Especially at low frequencies of 8 and 32 Hz, apparent resistivity anomalies are roughly electric dipolar in nature, with undershoots and overshoots with respect to ρ_a over the ends of the body for ρ_{xy} and over the sides for ρ_{yx} , respectively. These large anomalies are mainly caused by free charges occurring in the boundary between the body and the host layer. Such anomalous behavior due to this charge, when it occurs about conductive bodies, is referred to as current gathering (Wan-namaker et al., 1984b; Kim and Lee, 1994).

Behavior of impedance phases is entirely different from that of the apparent resistivities, as shown in Fig. 3. The overshoot-to-undershoot phenomenon with respect to layered-earth phases ϕ_a , which are labeled in the upper side of the figure, is observed at intermediate frequencies of 128 and 32 Hz. The layered-earth phases are increase with an increase of frequencies. The conductive body can be recognized with high impedance phase

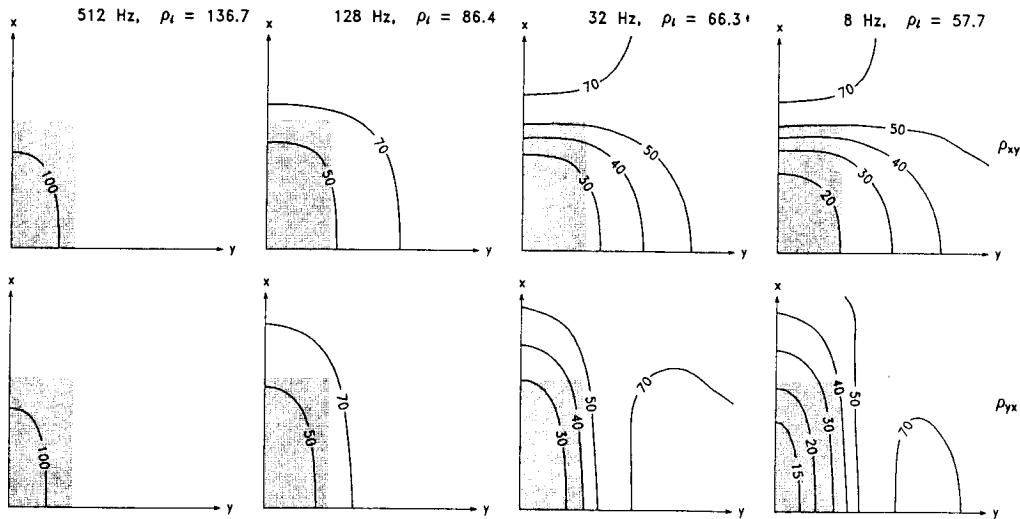


Fig. 2. Multifrequency plan maps of tensor apparent resistivities ρ_{xy} and ρ_{yx} over upper right-hand quadrant of the inhomogeneity of Fig. 1. The overburden resistivity is $500 \Omega \cdot m$, and the frequency and the layered-earth apparent resistivity ρ_l are given in the upper right-hand corner of each plot. The values of contour and ρ_l are in $\Omega \cdot m$.

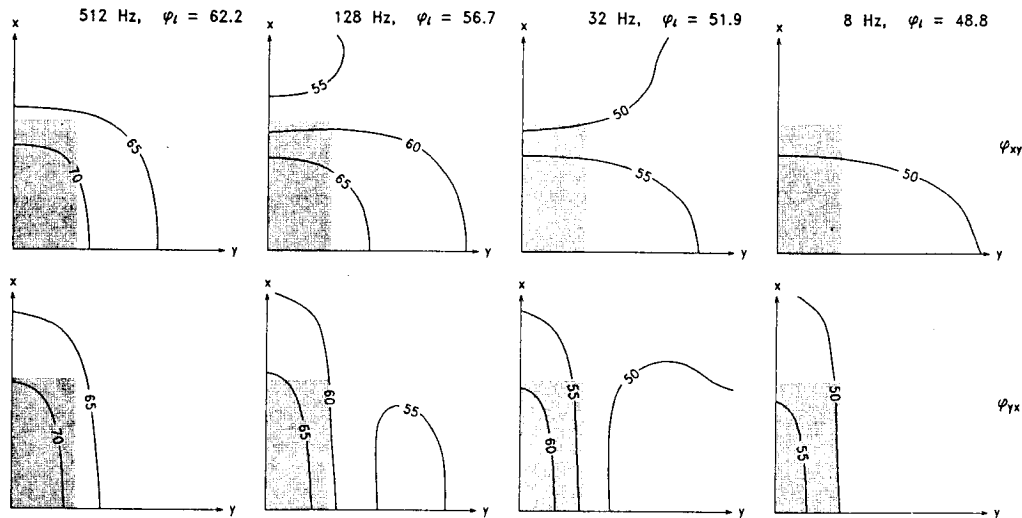


Fig. 3. Multifrequency plan maps of tensor impedance phases ϕ_{xy} and ϕ_{yx} for the resistive overburden of $500 \Omega \cdot m$.

anomalies. The impedance phases of ϕ_{xy} deviate greater than 10 degrees from at higher frequencies of 128 and 512 Hz. At 8 Hz, however, ϕ_{xy} deviates less than 3 degrees from ϕ_l , because the secondary electric field is essentially in phase with the incident electric field and total and incident magnetic fields are nearly equal. For ϕ_{yx} such small deviation occurs at 1 Hz (not shown).

Figs. 4 and 5 show apparent resistivities and impedance phases for the model with conductive overburden ($10 \Omega \cdot m$), respectively. Because electromagnetic energy

is more dissipated for the conductive overburden than for the resistive one, anomalies due to the conductive body in the host layer is greatly masked for the conductive overburden compared with the resistive one. Even at low frequency of 1 Hz the overshoot-to-undershoot behavior is not clear for the case of conductive overburden.

Fig. 6 illustrates the effect of overburden on tipper magnitudes. Upper and lower figures indicate the results for the conductive and resistive overburdens, respective-

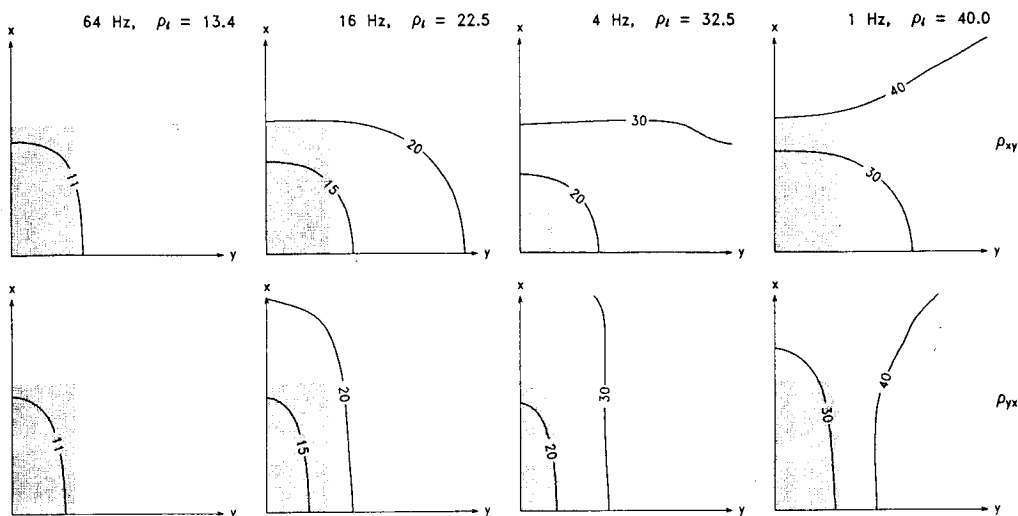


Fig. 4. Multifrequency plan maps of tensor apparent resistivities ρ_{xy} and ρ_{yx} for the conductive overburden of $10 \Omega \cdot m$.

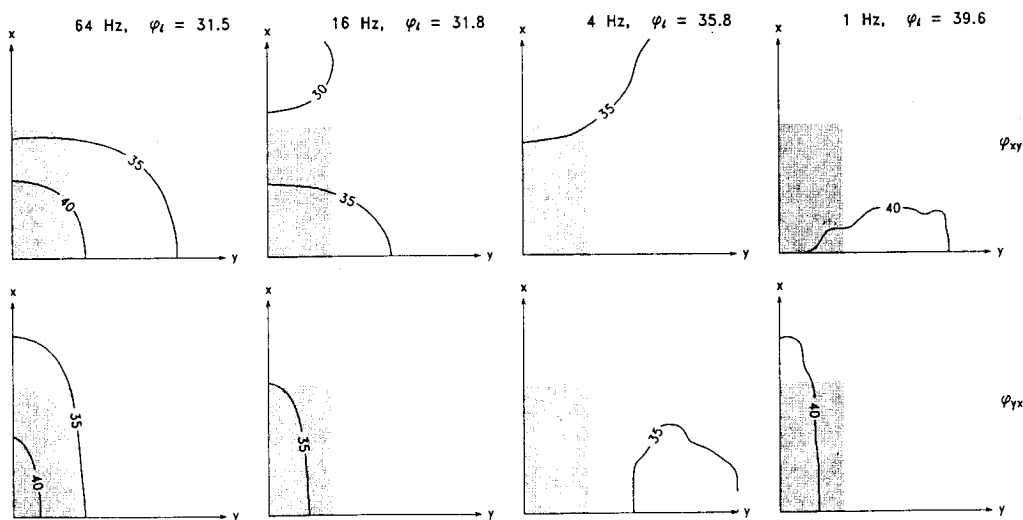


Fig. 5. Multifrequency plan maps of tensor phases ϕ_{xy} and ϕ_{yx} for the conductive overburden of $10 \Omega \cdot m$.

ly. Large amplitudes of tipper always occur over the sides of the body. Tipper magnitudes peak at 32 Hz for the conductive overburden and at 128 Hz for the resistive overburden. An effect of 1-D layering is less significant for tipper than for apparent resistivity and impedance phase. The maximum anomaly for the case of resistive overburden is only about twice for that of conductive overburden.

EFFECT OF BASEMENT RESISTIVITY

A model is given in Fig. 7 to show a model to explore

an effect of basement resistivities on MT responses of a 3-D prism. Shallow conductive prism of $5 \Omega \cdot m$ appears in an overburden overlain upon resistive and conductive basements. The size of prism is $300 \times 300 \times 600$ m, and its depth is 25 m. The first layer is 400 m thick and its resistivity is $50 \Omega \cdot m$.

The apparent resistivity signatures produced by the model structure shown in Fig. 7 with resistive basement ($500 \Omega \cdot m$) are displayed in Fig. 8. Especially at low frequencies of 1 and 8 Hz, the approximately electric dipolar character of apparent resistivities is apparent over the ends of the body for ρ_{xy} and over the sides for ρ_{yx} .

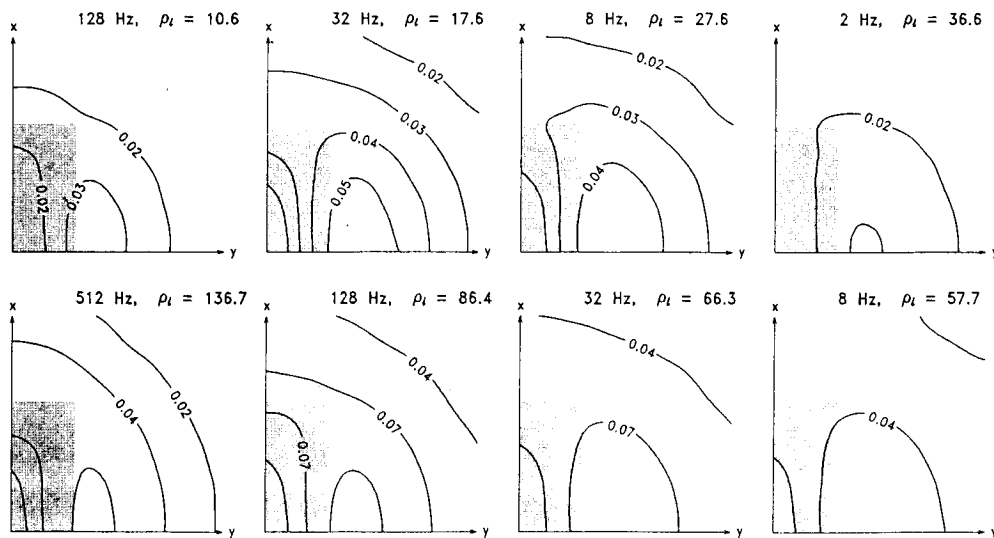


Fig. 6. Multifrequency plan maps of tipper magnitude $|T|$ for conductive (upper row) and resistive (lower row) overburden. The contours are dimensionless.

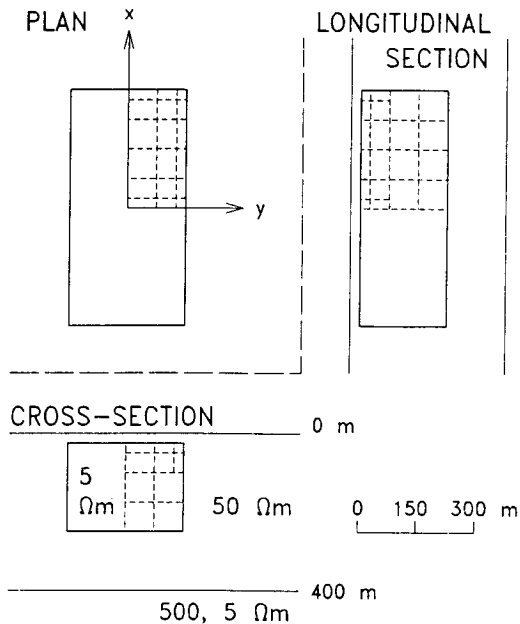


Fig. 7. Prismatic 3-D body in upper layer. Basement resistivities of 500 and 5 Ω·m are considered.

Boundary charges cause spatial apparent resistivity variation by a factor of nearly 25 for ρ_{yy} and 40 for ρ_{xx} , which is much higher than the resistivity contrast of the 3-D body to overburden. Such extremities are mainly due to the phenomenon that current gathering into conductive structure produces strong apparent resistivity anomalies

that actually increase to a low-frequency asymptote as frequency falls. At high frequencies of 64 and 512 Hz, the overshoot-to-undershoot behavior is not so obvious and apparent resistivities are smaller than layered-earth apparent resistivities.

Fig. 9 shows impedance phases for the model with resistive basement. At the high frequencies of 64 and 512 Hz, departures may appear in excess of 17 degrees from the layered host phase ϕ_0 , while at 1 Hz the impedance phases deviate less than 3 degrees from ϕ_0 . Impedance phase anomalies due to the conductive body, extraneous structure peaks at high frequencies, certainly in excess of 64 Hz, and contribute negligibly to observed phase responses below 1 Hz.

Apparent resistivities and impedance phases for the model with conductive basement (5 Ω·m) are displayed in Figs. 10 and 11, respectively. At higher frequencies, anomalies due to the 3-D body for the case of conductive basement are similar to those for the case of resistive basement. At lower frequencies, however, anomalies are much different between the two cases.

When the effect of basement resistivity is considered, two factors seem to be important. First, dissipation of EM waves in conductive media is greater than in resistive ones. Second, current perturbations about a 3-D body overlying a resistive basement tend to be confined to the less resistive upper layer. This leads to a geometric attenuation of the secondary fields with distance that is slower when a resistive basement is present than when a conductive one is. For example, the contribution of free

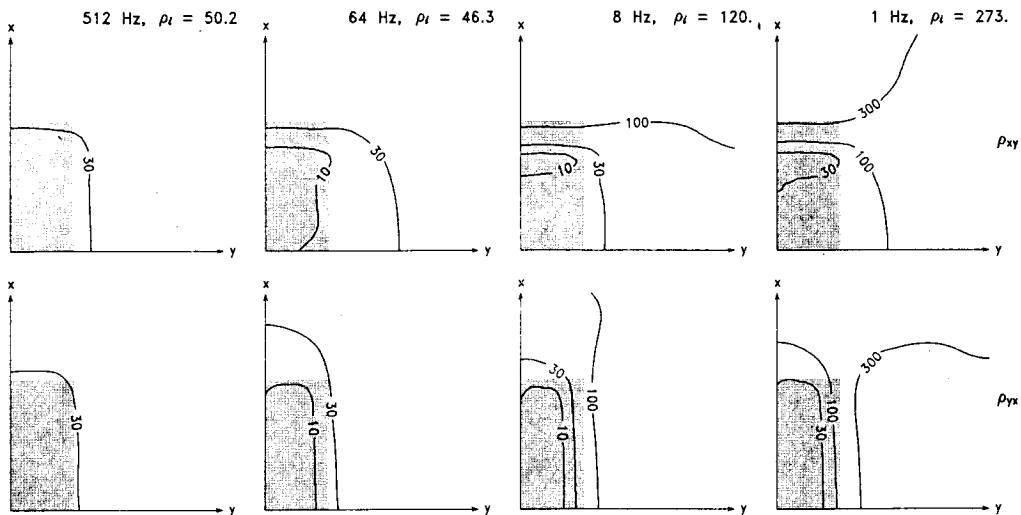


Fig. 8. Multifrequency plan maps of tensor apparent resistivities ρ_{xy} and ρ_{yx} for the resistive basement of $500 \Omega \cdot m$.

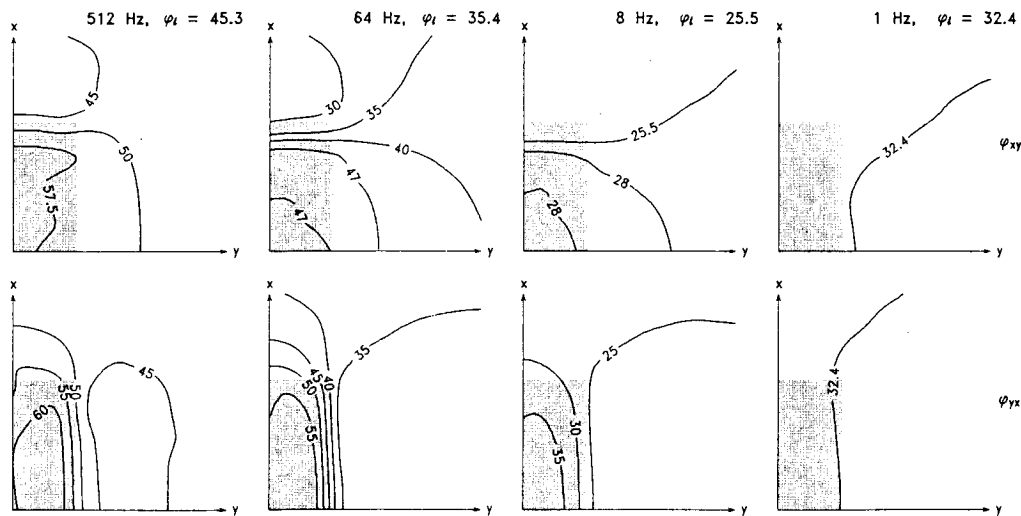


Fig. 9. Multifrequency plan maps of tensor impedance phases ϕ_{xy} and ϕ_{yx} for the resistive basement of $500 \Omega \cdot m$.

charge on the ends of the 3-D body to the secondary electric fields is stronger for a resistive basement than for a conductive one.

CONCLUSIONS

The calculations shown in this paper indicate that MT responses of 3-D conductive body are affected by the nature of 1-D layering. An effect of the layering is more significant for apparent resistivity and impedance phase than for tipper magnitude.

The effect of overburden on MT responses is to shade

the target from being detected. The shading effect is more apparent for conductive overburden than for resistive one, because the dissipation rate of EM waves is proportional to the conductivity of the medium. For resistive overburden apparent resistivity anomalies due to the conductive body at low frequencies are approximately electric dipolar character, with overshoots and undershoots with respect to layered-earth apparent resistivities. Similar overshoot-to-undershoot phenomenon occurs in impedance phase anomalies for resistive overburden but at higher frequencies. Tipper anomalies show only a small difference between for resistive overburden and for

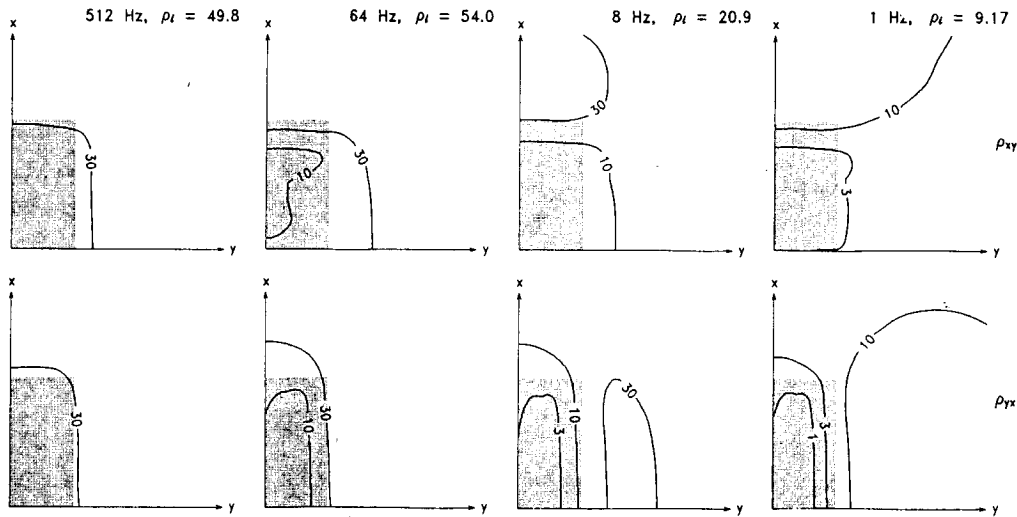


Fig. 10. Multifrequency plan maps of tensor apparent resistivities ρ_{xy} and ρ_{yx} for the conductive basement of $500 \Omega \cdot m$.

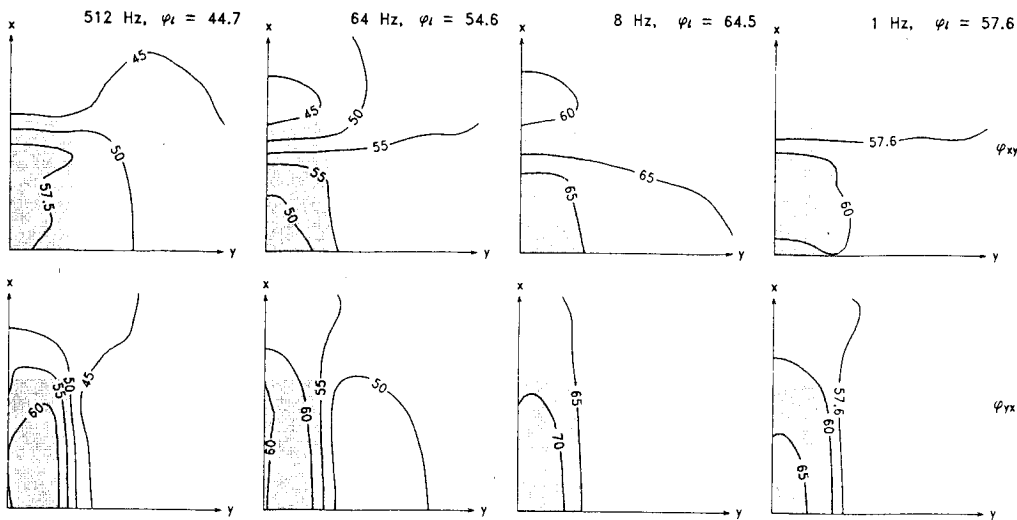


Fig. 11. Multifrequency plan maps of tensor impedance phases ϕ_{xy} and ϕ_{yx} for the conductive basement of $500 \Omega \cdot m$.

conductive one.

For a shallow conductive body strong MT anomalies with electric dipolar character are caused by boundary charges. The anomaly due to the conductive body in the upper layer is higher when a resistive basement is present than when a conductive one is. For the resistive basement current perturbations about the body tend to be confined to the less resistive upper layer.

ACKNOWLEDGEMENTS

This research was supported by the Korean Science

and Engineering Foundation and the Research Center for Mineral Resources. I wish to thank Dr. Seung-Hwan Chung for his critical reading of the manuscript.

REFERENCES

Das, U.C. and Verma, S.K. (1982) Electromagnetic response of an arbitrarily shaped three-dimensional conductor in a layered earth-numerical results. *Geophys. J. R. astr. Soc.*, v. 68, p. 55-66.
 Gamble, T.D., Goubau, W.M., and Clarke, J. (1979) Magnetotellurics with a remote reference. *Geophysics*, v. 47, p. 932-937.

- Keller, G.V. and Frischnecht, F.C. (1966) *Electrical Methods in Geophysical Prospecting*. Pergamon Press, 486 p.
- Kim, H.J. and Lee, D.S. (1994) Three-dimensional magnetotelluric modeling using integral equations. *Econ. Environ. Geol.*, v. 27, p. 191-199.
- Takasugi, S., Muramatsu, S., Yamaki, H. and Ikehama, T. (1992) Development of a high accuracy MT system-System design and noise test-. *Butsuri-Tansa*, v. 45, p. 190-203.
- Ting, S.C. and Hohmann, G.W. (1981) Integral equation modeling of three-dimensional magnetotelluric response. *Geophysics*, v. 46, p. 182-197.
- Vozoff, K. (1972) The magnetotelluric method in the exploration of sedimentary basins. *Geophysics*, v. 37, p. 98-141.
- Wannamaker, P.E., Hohmann, G.W. and SanFilipo, W.A. (1984a) Electromagnetic modeling of three-dimensional bodies in layered earths using integral equations. *Geophysics*, v. 49, p. 60-74.
- Wannamaker, P.E., Hohmann, G.W. and Ward, S.H. (1984b) Magnetotelluric responses of three-dimensional bodies in layered earths. *Geophysics*, v. 49, p. 1517-1533.
- Wannamaker, P.E. (1991) Advances in three-dimensional magnetotelluric modeling using integral equations. *Geophysics*, v. 56, p. 1716-1728.

Manuscript received 31, August 1994

3차원체의 MT응답에 미치는 층상대지의 효과

김희준 · 홍철훈

요 약: 2층구조 대지속에 존재하는 유한 크기의 불균질체로 인한 지자기 지전류 (MT) 응답을 적분방정식법으로 계산하였다. 적분방정식은 입사전자장과 3차원물체 내부의 산란전류를 층상대지에 적합한 전기적 텐서 그린함수를 통하여 연결시킨다. 본 논문에서는 3차원체의 MT응답에 미치는 표층과 기반층의 영향에 대하여 검토하였다. 표층은 탐사대상물의 검출을 방해하는 효과를 가지며 그 효과는 표층의 전기비저항이 높을 때보다 낮을 때가 더 뚜렷하다. 한편 기반은 상층의 3차원체에 의한 MT이상을 높이는 효과를 가져올 수도 있다. 전기비저항이 높은 기반이 존재하면 물체에 의한 전류의 미소변동은 보다 전기비저항이 낮은 상층에 한정되는 경향이 있다.